[4] GOLDBURG, W. I., and HUANG, J. S., 1975 *Fluctuations, Instabilities and Phase Transitions*, edited by T. Riste, Nato ASI Series B, Vol. 11 (Plenum), p. 87.
[5] CAHN, J. W., 1961, *Acta metall.*, **9**, 795.
[6] EVANS, R., 1979, *Adv. Phys.*, **28**, 143.
[7] EBNER, C., SAAM, W. F., and STROUD,D., 1976, *Phys. Rev.* A, **14**, 2264.
[8] TELO DA GAMA, M. M., and EVANS, R., 1979, *Molec. Phys.*, **38**, 367.
[9] ABRAHAM, F. F., 1976, *J. chem. Phys.*, **64**, 2660.
[10] COOK, H. E., 1970, *Acta metall.*, **18**, 297.
[11] ABRAHAM, F. F., SCHREIBER, D. E., MRUZIK, M. R., and POUND, G. M., 1976, *Phys. Rev. Lett.*, **36**, 261.
[12] MRUZIK, M. R., ABRAHAM, F. F., and POUND, G. M., 1978, *J. chem. Phys.*, **69**, 3462.
[13] ABRAHAM, F. F., MRUZIK, M. R., and POUND, G. M., 1979, *J. chem. Phys.*, **70**, 2577.

MOLECULAR PHYSICS, 1979, VOL. 38, No. 3, 699–716

Studies of molecular motions and vibrational relaxation in acetonitrile

IV. Far-infra-red and molecular dynamics in carbon tetrachloride solution

by M. W. EVANS and G. J. EVANS
Edward Davies Chemical Laboratory, U.C.W. Aberystwyth, Dyfed, Wales
J. YARWOOD and P. L. JAMES
Department of Chemistry, University of Durham, Durham City, England
and R. ARNDT
Institüt für Physikalische Chemie,
Techn. Universität, Braunschweig, W. Germany

(*Received* 17 *November* 1978)

Far-infra-red spectra in the 2–200 cm^{-1} region of dilute solutions of CH_3CN in CCl_4 solution have been employed to test the various analytical models available for the description of rotational motions of a symmetric top dipole in the liquid phase. It is found that none of the various approximants of the Mori continued fraction description of reorientational correlation function fit the experimental data satisfactorily. This implies that, although the data (from this and other techniques) may appear to be properly described by a simple rotational diffusion model at long times, the short time dynamics are too complicated to be reproduced even by much more sophisticated models. The data are able to clearly discriminate between the various models tried and, in addition, give valuable information about the nature and extent of the mean square torques acting on the probe molecule.

1. INTRODUCTION

The problem of describing analytically the molecular dynamics and interactions in a dense fluid of dipolar molecules may be approached using a wide range of spectroscopic methods [1–3]. These include infra-red, far-infra-red and microwave absorption, Raman and Rayleigh light scattering, neutron scattering, and nuclear magnetic resonance techniques. (There have recently been several excellent reviews of the subject [1–4].) A viable model of the dynamical evolution of the N molecules from an arbitrary initial time, $t = 0$, must then be capable of describing the various spectroscopic features in a consistent manner. In other words, it must be consistent with *all* the data and must allow such data to be expressed in physical terms which are suitable for intercomparison. It has become clear recently [2, 5] that models described in terms of inverse frequencies (such as the Debye relaxation time [6] or the time between collisions of extended diffusion theory [7]) lead to disparate and contradictory results for extensively studied [5, 8] liquids such as CH_2Cl_2. The fundamental reason for this is that

0026-8976/79/3803 0699 $02.00

the models involved approximate the Liouville equation [3, 8] of motion too roughly. Most, if not all, these models are early approximants (or truncations) of the Mori continued fraction [8–10] expansion of the Liouville equation and, as such, define the potential energy of the total hamiltonian using only one or two terms, in the effective Taylor expansion [3, 4 (b)]. For example, in the *J*-diffusion model [3, 7, 11] even the mean square torque, the first derivative of the potential energy with respect to orientation, is not defined. Furthermore, this is true for any model which relies on the concept of an elastic collision regardless of the type of underlying statistics employed [12].

This situation will remain unless a realistic intermolecular potential is employed, either by direct numerical integration of the equations of motion [13] (molecular dynamics simulation) or by taking a fundamentalist line in employing later approximants of various continued fractions. We describe here a method for the evaluation of the mean square torque acting on a dipolar molecule and its derivative using the truncated Mori expansion of the orientational autocorrelation function $C_u(t) = \langle \mathbf{u}(0) \cdot \mathbf{u}(t) \rangle$ ($\mathbf{u}$ is a dipole unit vector) without recourse to least mean squares fitting [10 (a)] to the observed far-infra-red spectra. This technique is applied to the analysis of data on dilute solutions of acetonitrile in a range of solvents by observing the peak frequencies of both the dielectric loss, $\epsilon''(\omega)$, and the power absorption, $\alpha(\omega)$, spectra. We express some currently popular models in terms of Mori approximants and evaluate them using the 0-THz frequency spectra for the same solutions. In this way we are able to discriminate, in a very powerful manner, the relative validities of the assumed models. In order to counteract the complexity of the overall dynamics in an isotropic fluid we have also studied the far-infra-red spectrum of CH_3CN in a solvent which forms a cholesteric phase (and which therefore restricts, to some extent, the freedom of molecular motion).

2. General theoretical background

The starting point is the model-independent Mori equation of motion [15–17] of a dynamical array of N interacting molecules, viz.

$$\dot{\mathbf{A}}(t) = i\Omega_{\mathbf{A}}\mathbf{A}(t) - \int_0^t K_{\mathbf{A}}(t-\tau)\mathbf{A}(\tau)\, d\tau + \mathbf{F}_{\mathbf{A}}(t), \tag{1}$$

where $\mathbf{A}_j(t)$ are the n linearly independent variables and $\Omega_{\mathbf{A}}$ is a resonance frequency operator. The matrix $K_{\mathbf{A}}$ is a memory function and $\mathbf{F}_{\mathbf{A}}(t)$ is a random force or torque which is Mori-propagated from $\mathbf{A}(0)$ and is a generalized stochastic variable [16]. Physical realization of equation (1) may be expressed through the following models which have often been used in the interpretation [1–4] of infra-red, Raman, N.M.R., (spin–spin, nuclear quadrupole and spin–lattice relaxation) and neutron scattering data.

(1) When the memory kernel $K_{\mathbf{A}}$ has delta function components (i.e. $K_0(t) = D\delta(t)$) equation (1) reduces to the Langevin equation [15 (b)] for an asymmetric top, solved very recently by Morita [18]. This represents the inertia-corrected asymmetric top analogue of the Debye model of rotational diffusion (infinitely small reorientations taking place infinitely rapidly). The solution leads to friction coefficients [17 (d)] β_{xx}, β_{yy} and β_{zz} along the principal inertial axes and they may be found using the shape factor analysis of Büdo *et al.* [19].

For a symmetric top molecule $\beta_{xx} = \beta_{yy}$ and, since the friction coefficients are obtained from the maximum in the dielectric loss curve, the two β values can be obtained without the use of adjustable parameters (see equation (7)).

(2) The next simplest model is characterized [20 (a)] by writing

$$K_0(t) = {}^{FR}K_0(t) \exp(-|t|/\tau_\omega), \tag{2}$$

where τ_ω is the correlation time of the dynamical system and ${}^{FR}K_0(0)$ the memory kernel for a maxwellian ensemble of non-interacting rotors. This model corresponds to the Gordon *J*-diffusion model [7] for instantaneous, elastic collision-interrupted free rotations or to the Chandler binary collision model [20 (b)]. The resulting spectrum (the Fourier transform of $\langle \boldsymbol{\omega}(0) \cdot \boldsymbol{\omega}(t) \rangle$, where ω is the angular velocity about the dipole axis) is therefore analytically identical [21] with that obtained using the *J*-diffusion model. Equation (2) represents a first order approximant of the Mori continued fraction [9, 10].

(3) More complicated, but tractable, expressions for the dipole orientational correlation [8 (b)] function $C_u(t)$ may be obtained [10] using other approximants of the Mori continued fraction expansion. The rate of convergence of successive terms to the Liouville equation

$$\dot{\mathbf{u}} = i\mathscr{L}\mathbf{u} \tag{3}$$

is, however, (at present) unknown.

Truncations at second- and third-order respectively [8, 10, 22] lead to the approximants defined by,

$$K_u^{(1)}(t) = K_u^{(1)}(0) \exp(-[\pi K_u^{(1)}(0)/2]^{1/2}\, t) \equiv K_u^{(1)}(0) \exp(-\gamma_1 t) \tag{4}$$

and

$$K_u^{(2)}(t) = K_u^{(2)}(0) \exp(-[\pi K_u^{(2)}(0)/2]^{1/2}\, t) \equiv K_u^{(2)}(0) \exp(-\gamma_2 t), \tag{5}$$

where $K_u^{(1)}(t)$ and $K_u^{(2)}(t)$ are the second and third memory functions of $C_u(t)$. In previous publications [10, 14 (a)] the γ_1 and γ_2 factors in (4) and (5) have been treated as adjustable parameters but, as is made clear later (and elsewhere [8]) the equilibrium averages $(K_u^{(0)}(0), K_u^{(1)}(0))$ and $(K_u^{(0)}(0), K_u^{(1)}(0), K_u^{(2)}(0))$ (depending on the approximant used) may be calculated (without need for least squares fitting) from the maxima of the dielectric loss ($\epsilon''(\omega)$) and power absorption ($\alpha(\omega)$) curves in the 0-THz frequency region. Furthermore, only one set of experimental data is needed (provided refractive index data are available [14 (c)]) since the relationship

$$\alpha(\tilde{\nu}) = 2\pi\epsilon''(\tilde{\nu})\tilde{\nu}/n(\tilde{\nu}) \tag{6}$$

can be used. The memory functions mentioned here are, of course, closely related to the dynamics and interactions of the molecules in the fluid [10, 23, 24] and their determination can throw considerable light on these molecular properties. $K_u^{(0)}(0)$ is proportional to the orientational second moment ($2kT/I_B$ for a symmetric top molecule), $K_u^{(1)}(0)$ is related [24] to the mean square torque, $\langle O(V)^2 \rangle$, while $K_u^{(2)}(0)$ is related to the torque and to its mean squared time derivative.

(4) Finally one may use an itinerant libration model as developed by Coffey *et al.* [17]; details of which are presented fully elsewhere [17]. This is a zeroth approximant of the *matrix* Mori series considered by Damle *et al.* [25] for a translational itinerant oscillator in the context of neutron scattering. In particular, [8 (a)] the memory function $K_{\mathbf{A}}$ of equation (1) is given by

$$K_{\mathbf{A}}=\begin{bmatrix}\beta_2\delta(t)+\omega_0^2 & -\omega_0^2\\ -\Omega_0^2 & \beta_1\delta(t)+\Omega_0^2\end{bmatrix}, \tag{7}$$

where $\omega_0^2=K_u^{(0)}(0)$ and $\Omega_0^2=K_u^{(1)}(0)=(I_2/I_1)K_u^{(0)}(0)$ in this notation, β_1 and β_2 are friction coefficients. The librating disc-like molecule is situated [17 (b)] in a rigid annulus (cage) of neighbouring molecules, both disc and annulus being free to rotate about a central axis perpendicular to their plane. I_1 and I_2 are the moments of inertia of the disc and annulus respectively. The parameters of this model [17], with one exception, may be identified with measurable frequencies such as those of the dielectric loss and power absorption. The adjustable parameter, β_2, is defined as the hydrodynamic friction between the librating/diffusing molecule and the annulus of surrounding molecules. Analytical tractability is only achieved for planar reorientations of the symmetric top dipolar axis. In general, however, this restriction may be lifted by using numerical methods (computer simulations) [26] or by noticing that the stochastic equations of motion governing the system may be identified with those developed by Budó [19] for the brownian motion of a molecule carrying a pair of interacting dipoles. However, this dipole–dipole coupling mechanism, whilst surely being important for pure dipolar liquids, should be much reduced or even negligible at the very low concentrations used in this work (in order to attempt to avoid the problem of ignoring the internal field [27 (a)] and to eliminate cross correlation effects on $C_u(t)$). We investigate here the effect of β_2 on the low frequency (theoretical) power absorption profile.

3. Definition of the variables of model 3

The analytical expression [10 (a)] for the power absorption coefficient of the two variable approximant (equation (4)) is

$$\alpha(\omega)=\frac{A\omega^2\,K_u^{(0)}(0)K_u^{(1)}(0)\gamma}{\gamma^2[K_u^{(0)}(0)-\omega^2]^2+\omega^2[\omega^2-(K_u^{(0)}(0)+K_u^{(1)}(0))]^2}. \tag{8}$$

If this expression is differentiated we obtain $K_u^{(1)}(0)$ in terms of the maximum frequency, ω_1, of the $\alpha(\omega)$ curve, viz.

$$K_u^{(1)}(0)=\frac{4\omega_1^4(\omega_1^2-K_u^{(0)}(0))}{\pi(K_u^{(0)}(0)-\omega_1^2)(K_u^{(0)}(0)+\omega_1^2)+4\omega_1^4}. \tag{9}$$

Thus the mean square torque can be measured directly from the infra-red peak frequency, this band shifting to higher frequency as the torque increases.

By differentiating the corresponding expression for the dielectric loss $\epsilon''(\omega)$ we arrive at the useful approximation

$$K_u^{(1)}(0)=\frac{\pi}{2}\left[\frac{2kT\tau_D}{I_B}\right]^2, \tag{10}$$

where τ_D is the inverse of the dielectric loss peak frequency, ω_0. τ_D may therefore be directly calculated through equation (10). In the next approximant the two equations,

$$\left[\frac{\partial\epsilon''(\omega)}{\partial\omega}\right]_{\omega=\omega_0}=0 \tag{11}$$

and

$$\left[\frac{\partial\alpha(\omega)}{\partial\omega}\right]_{\omega=\omega_1}=0, \tag{12}$$

are solved simultaneously to give $K_u^{(1)}(0)$ and $K_u^{(2)}(0)$. (The details of this solution are given in the Appendix.)

Needless to say, the $K_u^{(1)}(0)$ value estimated from equation (10) or from the pair of following equations should be the same were the truncated (continued) fraction already a reasonable approximant to $\dot{\mathbf{u}}=i\mathscr{L}\mathbf{u}$. By noticing that the far wing of the Rayleigh depolarized band decays [29] approximately as $\epsilon''(\omega)/\omega$, this method may be extended one step further to evaluate the set ($K_u^{(0)}(0)$, $K_u^{(1)}(0)$, $K_u^{(2)}(0)$ and $K_u^{(3)}(0)$) given the interrelations between the coefficients of time in the Maclaurin expansions of $C_u(t)$ [3, p. 18] and the correlation function appropriate to Rayleigh scattering, i.e. for simplest geometries $\frac{1}{2}\langle 3(\mathbf{u}(0)\,.\,\mathbf{u}(t))^2-1\rangle$. By this method we can move towards experimental consistency without recourse to modelling at too early a stage. It may also be possible to extend the set of $K_u^{(n)}(0)$ further in the future with aid of recent mathematical developments [27 (b)] in the ill-posed problem theory as a method of estimating the statistical information lost by using approximants.

4. Experimental

The far-infra-red measurements reported here for acetonitrile in solution in CCl_4 were made using a Beckman-R.I.I.C. Ltd. FS720 (20–250 cm^{-1}), Michelson interferometer equipped with a Golay (IR50) detector and a QMC Industrial Research Ltd. liquid helium cooled germanium bolometer (2–30 cm^{-1}). In the low frequency region the interferometer was converted to the Martin–Puplett [31] mode. The variable temperature cell unit was equipped with polyethylene windows and temperature control was via a Beckman R.I.I.C. Ltd. controller. It is estimated that spectra are reproducible to within ± 2 per cent in the 30–250 cm^{-1} region and within ± 1 per cent at frequencies between 2 and 30 cm^{-1}. Static permittivities were made with a W.T.W., Model DM01 dipolemeter while the refractive indices were obtained at the National Physics Laboratory using a special dispersive cell [32] developed there (these measurements will be described in detail elsewhere). Spectroscopic grade CH_3CN and CCl_4 were used throughout after drying over molecular sieves. Solutions were made up by volume immediately prior to measurement. Measurements on CH_3CN in cholesteryl oleyl carbonate were made using a Grubb Parsons/NPL Michelson interferometer equipped with Golay and helium cooled Indium/Antimonide detectors in order to cover the region between 1 and 250 cm^{-1}. A saturated solution of CH_3CN in this solvent was prepared by refluxing for 48 hours and separating layers. This yielded a solution with a mole fraction for CH_3CN of about 0·04.

5. Results

Measurements of CH_3CN in CCl_4 have been made over a mole fraction range of 0·018–0·37 and at temperatures between 252 K and 343 K. Some typical power absorption spectra are shown in figure 1. We concentrate here on model fitting spectra at the lowest concentrations (mole fractions of 0·018 and 0·06) for the reasons outlined previously. Figures 2 and 3 show the refractive index data, $n(\tilde{\nu})$, and a comparison of the $\alpha(\tilde{\nu})$ and $\epsilon''(\tilde{\nu})$ curves at these two concentrations and 318 K. The static (ϵ_0) and long wavelength (ϵ_∞) (i.e. $> 50\ cm^{-1}$) permittivities are summarized in table 1.

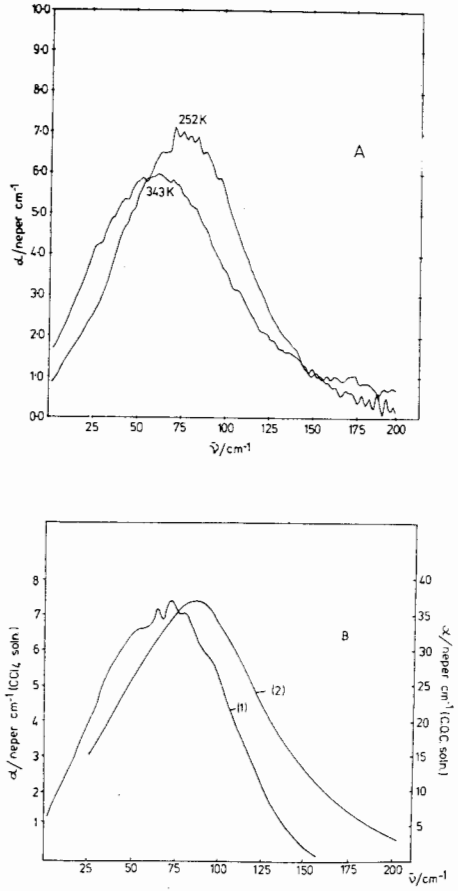

Figure 1. (A) Comparison of observed data for a mole fraction for CH_3CN in CCl_4 of 0·02 at two temperatures. (B) Comparison of observed data for CH_3CN in an isotropic phase (CCl_4) (1) and a mesomeric phase (cholesteryl oleyl carbonate, c.o.c.) (2) at comparable concentration and the same temperature.

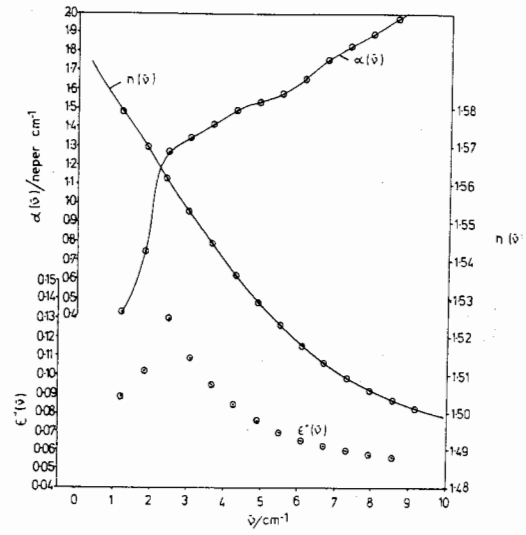

Figure 2. Low frequency observed $\alpha(\tilde{\nu})$, $n(\tilde{\nu})$ and $\epsilon''(\tilde{\nu})$ data for a mole fraction for CH_3CN in CCl_4 of 0·02 at 318 K.

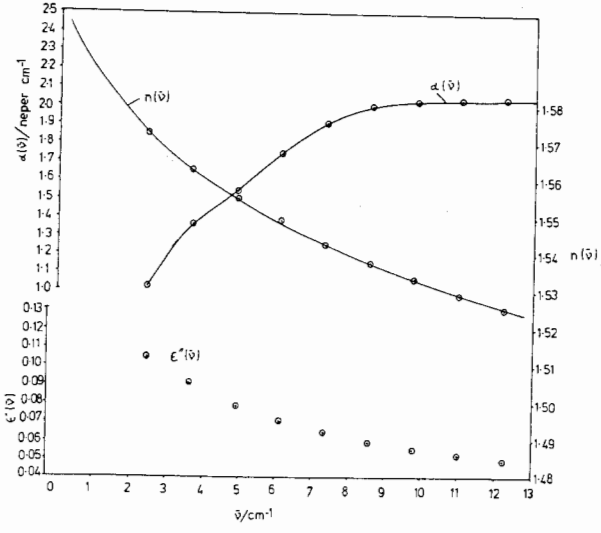

Figure 3. Low frequency observed $\alpha(\tilde{\nu})$, $n(\tilde{\nu})$ and $\epsilon''(\tilde{\nu})$ data for a mole fraction for CH_3CN in CCl_4 of 0·06 at 318 K.

Table 1. Permittivities and refractive index† of solutions of CH_3CN in CCl_4 (temperature‡ in K given as a superscript).

Mole fraction CH_3CN	ϵ_0^{318}	ϵ_0^{288}	ϵ_0^{252}	n_∞^{318}	n_∞^{288}	ϵ_∞^{318}	ϵ_∞^{288}	ϵ_∞^{252}
0·018	2·38	2·42	2·51	1·474	1·488	2·17	2·21	2·30
0·061	2·79	2·83	2·92	1·480	1·490	2·19	2·23	2·32

† At frequencies beyond 3 THz (100 cm^{-1}).

‡ Values of ϵ_0 and ϵ_∞ at 288 and 252 obtained from those measured at 318 K with $\partial\epsilon/\partial T = -0{\cdot}002$.

6. Evaluation of models and discussion

Before comparing our spectra with the models considered it is worth making the point that these models are applied in such a way that the microwave dielectric loss curve is reproduced accurately. This implies that, at long times, we *assume* in *each* case that the orientational correlation function, $\langle \mathbf{u}(0) \cdot \mathbf{u}(t) \rangle$, decays exponentially. This in turn ensures that the *short* time characteristics of each model (corresponding in the spectral domain to the high frequency, far-infra-red, region) may be individually compared with each other and with the experimental data. It has been emphasized [4, 8] that the great importance of far-infra-red data is that they provide a means of *discriminating* between different models *all of which* predict an exponential decay of the relevant correlation function at long times (and therefore all of which appear to fit the observed low frequency data equally well).

The models were fitted to the solutions of CH_3CN in CCl_4 which are respectively 1·8 and 6·1 per cent mole fraction in solute. We have assumed that the effects of collision induced dipoles and of cross correlations of the type, $\langle \mathbf{u}_i(0) \cdot \sum_{i \neq j} \mathbf{u}_j(t) \rangle$ (i and j referring to different molecules) are negligible at these very low concentrations. (Notice, however, evidence from Raman data [14 (a)] that dipole–dipole coupling [27] may be operative even at 2 per cent mole fraction.)

The delta function memory of model (1) is not able to produce a far-infra-red Poley absorption since the mean intermolecular potential energy is inaccurately defined (for example, its first derivative with respect to reorientation, the r.m.s. torque is undefined). This model therefore simply predicts a Debye plateau, [3, 4, 8] even when inertial corrections have been made [18] and this is the maximum value $\alpha(\tilde{\nu})$ reaches.

Figure 4 shows the observed spectrum at lowest concentration compared with those predicted by the J-diffusion or Chandler binary collision model (model 2) and with the planar itinerant oscillator (model 4). It is seen that the former is totally inadequate in that it peaks at the position predicted by the average rotational energy and makes no allowance for torques which shift the far-infra-red spectrum to higher frequency [3, 4, 8]. In other words, the J diffusion model merely broadens the $J+1 \leftarrow J$ pure rotational contour and again no evaluation of the mean square torque is possible. This is true even where the analytical statistics underlying this process of collision interrupted, free rotation

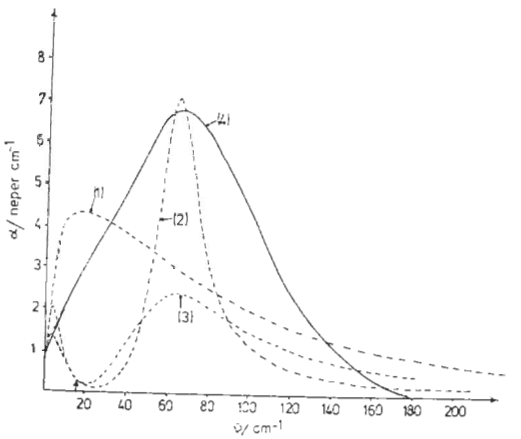

Figure 4. Comparison of observed and predicted data for CH_3CN in CCl_4 (0·02 mole fraction, 318 K). Curve (1), Binary collision (J diffusion) model first-order truncation; $\beta_1 = 20$ THz; Curve (2), Symmetric top itinerant oscillator model $I_1 = 10I_2$, $\beta_2 = 5$ THz; Curve (3), same with $\beta_2 = 15$ THz; Curve (4), observed data.

are generalized since the collisions are elastic and infinitely short. The r.m.s. torque is again undefined.

As in previous studies on highly polar molecules [8 (b), 17 (b, d)] the itinerant oscillator model produces a far-infra-red spectral distribution (figure 4) which is too narrow even for large values of the molecule–annulus friction parameter β_2 (figure 4). It is clear that fixing β_1 at $kT\tau_D/I_2$ (where τ_D is the inverse frequency of the loss peak) and varying β_2 does little to improve the situation (using $I_1 = 10I_2$ as one would expect [17 (b)]). Furthermore, the dipole–dipole coupling interpretation of equation (7) is not considered to be realistic for dilute solutions since such coupling should have been largely removed.

Figure 5 shows the results of comparing our observed data at 318 K with the higher order approximants of the Mori continued fraction (for example, equations (4) and (5)). It is seen that second- and successive-order continued fraction approximants of the orientational autocorrelation function, $C_u(t)$, first used by Barojas *et al.* [32] seem a little more realistic than models (1) and (2) which are respectively the zeroth- and first-order approximants to the continued fraction representation of the angular momentum autocorrelation function. Since we have approached these model calculations in several ways, it is worth outlining the methods used.

At first we had some difficulty in fitting our data to equation (8) since complete refractive index data were not available [14 (a)]. Initially we therefore fitted our $\alpha(\omega)$ data to an expression [23 (c, f), 14 (a)] which is independent of $n(\omega)$, viz.

$$\alpha(\omega) = \sqrt{(2)}\epsilon''(\omega)\omega/c[(\epsilon'(\omega)^2 + \epsilon''(\omega)^2)^{1/2} + \epsilon'(\omega)]^{1/2}, \qquad (13)$$

where $(\epsilon_0 - \epsilon_\infty)$ was fixed at the observed value (table 1). This equation gives

Table 2. Summary of parameters† obtained using second-order truncation of the Mori contained fraction.

Temperature/K	Mole fraction CH_3CN	$\bar{\nu}_1/cm^{-1}$	γ§	$K_u^{(1)}(0)$§	$\bar{\nu}_{max}$§	τ_D/ps§	τ_D/ps‡	τ_D (obs)‖
343	0·018	61 ± 2	4·4¶	26·5¶	72 ± 2¶	1·9¶	1·8	—
318	0·018	66 ± 2	3·0	21·0	68 ± 2	2·3	2·1	2·1
288	0·018	72 ± 2	2·7	24·1	73 ± 2	3·0	2·6	—
252	0·018	76 ± 2	2·6	32·9	82 ± 2	4·6	3·2	—
318	0·061	70 ± 2	7·9	59·2	88 ± 4	2·5	2·3	>2·6
288	0·061	73 ± 2	7·4	58·6	88 ± 4	2·8	2·7	—
252	0·061	80 ± 2	5·23	50·1	90 ± 4	3·6	3·4	—

† Given in terms of $x^{1/2}$ γ and $xK_u^{(1)}(0)$ where $x = I_B/2kT$.
‡ Calculated using equations (9) and (14)—see text.
§ Values obtained by fitting to equation (13) with $\epsilon_0 - \epsilon_\infty$ fixed at observed value (see table 1).
‖ τ_D measured off the $\epsilon''(\bar{\nu})$ versus $\bar{\nu}$ plots of figures 2 and 3—calculated using equation (6).
¶ Values obtained by fitting to equation (13) with (variable) $\epsilon_0 - \epsilon_\infty = 0{\cdot}29$; observed $(\epsilon_0 - \epsilon_\infty)$ not available at this temperature.

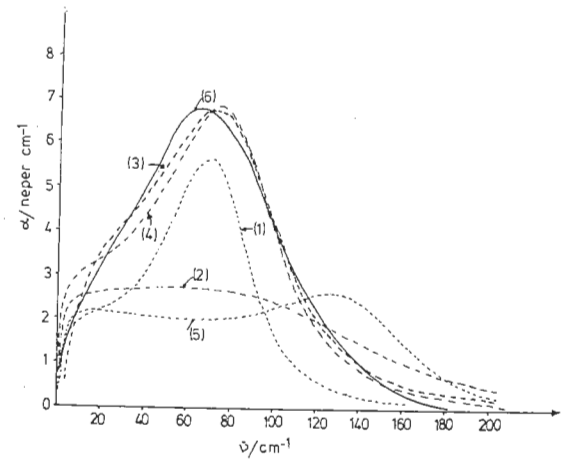

Figure 5. Comparison of observed (curve (6)) and predicted data for CH_3CN in CCl_4 (0·02 mole fraction, 318 K). Curve (1), second-order Mori truncation ; best fit to equation (13) with observed $\epsilon_0 - \epsilon_\infty = 0{\cdot}21$. Curve (2), second-order Mori truncation—values calculated using equations (9) and (14). Curve (3), second-order Mori truncation, best fit to equation (8) with variable $K^{u(0)}(0)$ and $\epsilon_0 - \epsilon_\infty$ see text for details. Curve (4) best fit to equation (13) with variable $\epsilon_0 - \epsilon_\infty$; $K_u^{(1)}(0) = 27{\cdot}5$, $\gamma = 3{\cdot}9$, $\epsilon_0 - \epsilon_\infty = 0{\cdot}33$. Curve 5, third-order Mori truncation, equations (A 1) and (A 2) with observed $\epsilon_0 - \epsilon_\infty$.

reasonably good fit (curve 1) with a maximum frequency somewhat higher than that observed (table 2). This result may be compared with that (curve 2) obtained when expressions (9) and (14) (see [22]) are used to calculate the two parameters $K_u^{(1)}(0)$ and γ without recourse to least squares fitting,

$$\gamma = \left[\frac{\pi}{2} K_u^{(1)}(0)\right]^{1/2}. \tag{14}$$

Clearly the fitting procedure is more satisfactory, at least, for this molecule. We then attempted to check the internal consistency of equations (8) and (13). Using the $\epsilon'(\omega)$ and $\epsilon''(\omega)$ data calculated by fitting to equation (14) we were able to recalculate the refractive index curve since

$$n(\omega) = \left\{\frac{(\epsilon''(\omega)^2 + \epsilon'(\omega)^2)^{1/2} + \epsilon'(\omega)}{2}\right\}^{1/2}. \tag{15}$$

This dispersion curve is shown in figure 6 (together with the experimental refractive index data obtained so far). As expected the curve shows a shallow minimum at $\sim 90\ cm^{-1}$ to high frequency of α_{max} at $\sim 66\ cm^{-1}$ (for a mole fraction of 0·018 at 318 K). The $n(\omega)$ data of figure 6 was then used to obtain a best fit to equation (8). Curve (3) of figure 5 shows the result of this fit allowing both $\epsilon_0 - \epsilon_\infty$ and $K_u^{(0)}(0)$ to vary. Although this fitted curve is in good agreement with the observed data it can only be achieved with a $K_u^{(0)}(0)$ value of 2·9 and $\epsilon_0 - \epsilon_\infty = 0{\cdot}55$. We then get a value of $\tau_D = 0{\cdot}66$ ps and the

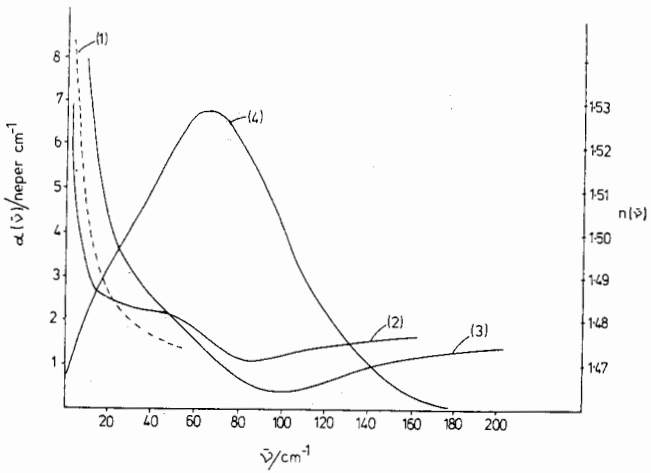

Figure 6. Refractive index and absorption data for a mole fraction for CH_3CN in CCl_4 of 0·02 (318 K). Curve (1), experimental data. Curve (2), calculated data using equation (15) with parameters calculated by a best fit to equation (13) (see table 5). Curve (3), calculated data using parameters calculated by a best fit to equation (8). Curve (4), experimental absorption spectrum.

calculated $\epsilon''(\omega)$ curve peaks at $\sim 8\ cm^{-1}$. Any attempt to fix $K_u^{(0)}(0)$ and/or $\epsilon_0 - \epsilon_\infty$ results in totally unreasonable low values of γ (leading to an extremely narrow band profile). The observed value of $\epsilon_0 - \epsilon_\infty$ is 0·21 (based on $\epsilon_\infty = n_\infty^2$; see table 1) and since $K_u^{(0)}(0)$ is already normalized to $I/2kT$ it should be fixed at a value of 1·0. The lack of consistency is thus a measure of the inadequacy of the model based on second-order truncation of the Mori continued fraction.

The next higher order approximant (equation 5) was then used to obtain $K_u^{(1)}(0)$, $K_u^{(2)}(0)$ and γ_2 (table 3) as outlined in the Appendix. Again there is significant deviation between observed and calculated data (curve (5)) and, clearly, convergence has still not been reached. This is reflected by the fact that $K_u^{(1)}(0) = 21{\cdot}0\, K_u^{(0)}(0)$ for the second approximant and $K_u^{(1)}(0) = 43{\cdot}2\, K_u^{(0)}(0)$ for the third approximant (tables 2 and 3). If this kind of continued fraction is to be physically meaningful (as opposed to useful) a means of extending it to infinity without introducing more adjustable variables must be found. One way in which this may be achieved is mentioned in § 3.

Table 3. Summary of parameters† obtained using third-order truncation to Mori continued fraction.

Temperature/ K	Mole fraction CH_3CN	γ	$K_u^{(1)}(0)$	$K_u^{(2)}(0)$	$\epsilon_0 - \epsilon_\infty$
318	0·018	10·0	43·2	64·1	0·21
318	0·061	10·6	48·7	72·4	0·60

† Units as in table 2.

Meanwhile, we have to make the point that the 0-THz absorption band of dipolar liquids eludes satisfactory analysis by the currently available analytical methods. The statistical mechanics of the autocorrelation function are too complicated even *without* taking into account the electrodynamics giving rise to the internal field problem. Attempts to reproduce the band shapes by varying phenomenological parameters for best fit are often unhelpful in that the underlying theoretical differences are obscured. However these empirical methods may be useful as the *only* available yardsticks when comparing data from different sources (see later).

In view of the significant discrepancies shown in figures 4 and 5 it is clear that inter-experimental comparisons will be meaningless if models such as these are used without great care. On the other hand, it is only by studying the high frequency (short time) regime of the orientational spectrum (correlation function) that we are able to discriminate *at all* between the various models. As mentioned previously (and as may be *seen* from figures 4 and 5) all the models considered here give excellent fits to the dielectric loss curve below $\sim 4\ cm^{-1}$ (i.e. in the low frequency, long time regime) but the physical meaning attributed to the relaxation times ($\tau_D = 1/\omega_{max}$ of the $\epsilon''(\omega)$ curve) will all be different. Each of the other techniques available for the measurement of τ_{1R} has associated with it significant drawbacks in this respect. The N.M.R. spin–spin relaxation technique, for example, gives information only about the area under the appropriate autocorrelation function and not the details of its decay. It is therefore usual to use the rotational diffusion model for calculating N.M.R. correlation times, the results being apparently reasonable only because the details of the ensemble molecular dynamics (embodied in figures 4 and 5) are obscured (and models which give the same overall relaxation times cannot, in any case be distinguished). In principle, infra-red and Raman studies of vibrational–rotational band broadening can be used to obtain information about the short time regime. In practice, however the bands have to be carefully chosen to avoid overlap in the wings with other (including hot band) transitions. Isotope effects and vibration–rotation coupling are also complicating features and it is rarely possible to achieve high enough signal/noise ratios in the high frequency regime. Likewise, since the far wings of the depolarized Rayleigh scattering [29] measures approximately the factor $\epsilon''(\omega)/\omega$, the short time details are clearly seen only with careful intensity control.

In view of the fact that most of the τ_{1R} data in the literature were obtained using information from the long time regime it is rather suprising that agreement between data from different techniques is difficult to find (tables 2 and 4). However, in comparing data from different techniques it is important to remember the following points (1) data obtained from depolarized Rayleigh scattering [35] or from dielectric relaxation measurements [36] in the *liquid* phase include contributions from cross correlations (i.e. correlation between the motions of neighbouring molecules); (2) that some of the data obtained from Raman and infra-red measurements are erroneous [33], either because the vibrational part of the band was not properly accounted for [43] or because the band profiles used [38, 39, 41] were disturbed by hot bands (this is particularly true [33] of the ν_2 and ν_4 bands). In his review of the extensive data for this molecule Griffiths [33] came to the conclusion that the best values for $\tau_{1R}(\perp)$ and $\tau_{2R}(\perp)$ were 3·3 and 1·1 ps respectively (at 298 K) which is (conveniently) exactly the

Table 4. Summary of reorientational correlation times† obtained for CH_3CN.

Liquid phase τ_{1R}/ps	Temperature/K	Technique	Reference	τ_{2R}/ps	Temperature/K	Technique	τ_D/ps	Temperature/K	Reference
3·2, 3·3	298	$IR(\nu_4)$	[42, 43]	2·0 ± 0·2	252	$R(\nu_2, \nu_3)$			[37]
				1·5 ± 0·2	286	$R(\nu_2, \nu_3)$			[37]
1·1, 1·5	308	$IR(\nu_2, \nu_4)$	[41]	1·2–1·4	293	$R(\nu_1, \nu_2, \nu_3, \nu_4)$			[38]
				1·1, 1·4	294	$R(\nu_2)$, N.M.R.			[39]
				1·5 ± 0·3, 1·2	296	$R(\nu_2)$, N.M.R.			[35, 40]
				0·9, 1·8	298	$R(\nu_1)$, Rayleigh			[34, 35]
				1·4	309	$R(\nu_2)$			[41]
				1·2 ± 0·1	318	$R(\nu_2, \nu_3)$			[37]
				0·7 ± 0·1	343	$R(\nu_2)$			[37]
							3·8 (microwave)	303	[36]
							3·1	323	[36]

Solutions τ_{1R}/ps	Solvent‡	Temperature/K	Technique	Reference	τ_{2R}/ps	Solvent‡	Temperature/K	Technique	Reference
2·3 ± 0·1	CCl_4 (1·8)	318	Far I.R.	[14 (a)]	2·0 ± 0·2	CCl_4 (3)	288	$R(\nu_2)$	[37]
2·2 ± 0·1	CCl_4 (6·0)	318	Far I.R.	[14 (a)]	2·1 ± 0·2	CCl_4 (6)	288	$R(\nu_2)$	[37]
2·8 ± 0·1	CCl_4 (1·8)	288	Far I.R.	[14 (a)]	1·9 ± 0·2	CCl_4 (16)	288	$R(\nu_2)$	[37]
2·6 ± 0·1	CCl_4 (6·0)	288	Far I.R.	[14 (a)]	2·6 ± 0·2	CCl_4 (37)	288	$R(\nu_2)$	[37]
7·6 ± 0·5	CCl_4 (25)	297	Microwave	[48]					
6·3 ± 0·5	CCl_4 (25)	313	Microwave	[48]					
4·5 ± 0·5	CCl_4 (25)	333	Microwave	[48]					
6·7 ± 0·5	Bz (25)	297	Microwave	[48]					
4·5 ± 0·5	Bz (25)	313	Microwave	[48]					
3·1 ± 0·5	Bz (25)	333	Microwave	[48]					

† Values are those obtained for rotation of the principal axis (i.e. τ_1).
‡ Concentration in mole per cent given in brackets.

ratio expected theoretically [44] for rotational diffusion. There is evidence, however, that both of these values may be incorrect. The τ_{1R} value is obtained from microwave data on the liquid and includes the effects of cross correlations. Data on τ_{2R} obtained from more recent measurements on ν_2 and ν_3 of acetonitrile suggest a value nearer 1·4 ps at 298 K (see table 4). Thus our τ_{1R}/τ_{2R} ratios which, for dilute solutions, lie in the 1·2–2·0 region (assuming that the temperature dependence of τ_{2R} is the same in CCl_4 as it is in the pure liquid) are probably not at variance with previous data. In any case, our far-infra-red data demonstrate conclusively that such a model is hopelessly inadequate to explain the details of molecular motion in the short time regime (a regime which *cannot* be studied properly using *any* of the other techniques currently employed). One possible way of making further progress in comparing the dynamics in the two time regimes would be to undertake an extensive molecular dynamics simulation of CH_3CN using a suitable empirical intermolecular potential. At the same time we should attempt to proceed analytically by approximating more realistically, using advanced statistical techniques, the Liouville equation for $\mathbf{u}$ or $\boldsymbol{\omega}$.

Table 5. Far-infra-red peak frequencies for CH_3CN solutions.

Solvent	Temperature/K	Mole fraction CH_3CN	ν_{max}/cm^{-1}	Reference
CCl_4	343	0·018	61 ± 2	This work
CCl_4	318	0·018	66 ± 2	This work
CCl_4	252	0·018	76 ± 2	This work
CCl_4	338	0·061	65 ± 2	This work
CCl_4	318	0·061	70 ± 2	This work
CCl_4	252	0·061	82 ± 3	This work
Cyclohexane	296	dilute soln.	~ 50	[45]
Carbon disulphide	314	2 per cent volume	~ 60	[46]
n-heptane	314	2 per cent volume	~ 38	[46]
CH_3CN	314	1·0	75 ± 5, 90 ± 2	[46, 49]
Cholesteryl oleyl carbonate	298	0·04	83 ± 2	This work

Finally, as mentioned previously, the far-infra-red data give, in principle, information about the intermolecular mean square torque. The simplest way to obtain a feeling for such torques is to notice that equation (9) gives an increased torque parameter $K_{\omega}^{(1)}(0)$ as the maximum frequency of the $\alpha(\omega)$ curve increases. Table 5 summarizes the ω_{max} data which have been obtained so far including data (see figure 1 (b)) in cholesteryl oleyl carbonate (which when pure, forms a cholesteric mesophase). It is rather obvious that the short time torsional oscillation of the CH_3CN even in isotropic phases is significantly environment sensitive. The mean square torques appear to increase on decreasing the temperature (large shifts occur, for example, when CH_2Cl_2 is frozen to the glassy state [47]) and also to increase when the number of acetonitrile molecules in the mixture increases. This provides direct evidence that molecular interactions

(presumably dipolar in origin) have a significant influence on the molecular distribution even in dilute solutions. Furthermore, it appears likely that such torques are smaller in hydrocarbon solvents (such as *n*-heptane) and much larger in mesomeric phases.

Thanks are due to Beckman-R.I.I.C. Ltd. and S.R.C. for equipment grants, for a C.A.S.E. studentship (to P.L.J.) and a research Fellowship (to G.J.E.). This work was also supported by a research grant from N.A.T.O. M.W.E. thanks the Ramsay Memorial Trust for the 1976–78 Fellowship.

Appendix

For third-order truncation of the Mori continued fraction,

$$\epsilon''(\omega)=(\epsilon_0-\epsilon_\infty)\omega K_u^{(0)}(0)K_u^{(1)}(0)K_u^{(2)}(0)[\pi K_u^{(2)}(0)/2]^{1/2}/D, \qquad (A\,1)$$

where

$$D=\pi/2K_u^{(2)}(0)\omega^2[\omega^2-(K_u^{(0)}(0)+K_u^{(1)}(0))]^2 + [\omega^4-\omega^2(K_u^{(0)}(0)+K_u^{(1)}(0)+K_u^{(2)}(0))+K_u^{(0)}(0)K_u^{(2)}(0)]^2$$

and

$$\alpha(\omega)=\frac{\omega\epsilon''(\omega)}{n(\omega)c}. \qquad (A\,2)$$

In the region where $\alpha(\omega)$ reaches a maximum, the refractive index $n(\omega)$ is constant to within a few per cent (figures 2 and 3) so that differentiation of (A 1) and (A 2) according to equations (11) and (12) yields the expressions

$$K_u^{(2)}(0)=\frac{\pi/2\omega_0^2[(K_u^{(0)}(0)+K_u^{(1)}(0))^2 - 2\omega_0^2 K_u^{(0)}(0)(K_u^{(0)}(0)+K_u^{(1)}(0))]}{K_u^{(0)}(0)(K_u^{(0)}(0)+2\omega_0^2)} \qquad (A\,3)$$

and

$$[K_u^{(2)}(0)]^2([K_u^{(0)}(0)]^2-\omega_1^4)+\omega_1^4 K_u^{(2)}(0)[\omega_1^2(4-\pi)+K_u^{(0)}(0)(\pi-4) + K_u^{(1)}(0)(\pi-2)]+[\omega_1^4-\omega_1^2(K_u^{(0)}(0)+K_u^{(1)}(0))][\omega_1^2(K_u^{(0)}(0) + K_u^{(1)}(0))-3\omega_1^4]=0. \qquad (A\,4)$$

By solving these equations simultaneously a quartic is developed in $K_u^{(1)}(0)$ which may be solved numerically. The quartic is

$$A[K_u^{(1)}(0)]^4+B[K_u^{(1)}(0)]^3+C[K_u^{(1)}(0)]^2+DK_u^{(1)}(0)+E=0, \qquad (A\,5)$$

where

$$A=a^2([K_u^{(0)}(0)]^2-\omega_1^4),$$

$$B=a\{2b[K_u^{(0)}(0)]^2+\omega_1^4[\pi-2(1+b)]\},$$

$$C=[K_u^{(0)}(0)]^2(b^2+2ac)+\omega_1^4[a(4-\pi)(\omega_1^2-K_u^{(0)}(0))+b(\pi-2) - b(b^2+2ac+1)],$$

$$D=2bc[K_u^{(0)}(0)]^2+\omega_1^4\{b(4-\pi)(\omega_1^2-K_u^{(0)}(0))+c[\pi-2(1+b)] +4\omega_1^2-2K_u^{(0)}(0)\},$$

$$E=c^2[K_u^{(0)}(0)]^2+\omega_1^4\{(4-\pi)(\omega_1^2-K_u^{(0)}(0))c-c^2 -(3\omega_1^4-4\omega_1^2 K_u^{(0)}(0)+[K_u^{(0)}(0)]^2)\}$$

and

$$a=\frac{\omega_0^2\pi}{2K_u^{(0)}(0)(K_u^{(0)}(0)+2\omega_0^2)},$$

$$b=\frac{(\pi-2)\omega_0^2}{K_u^{(0)}(0)+2\omega_0^2},$$

$$c=\frac{K_u^{(0)}(0)\omega_0^2}{K_u^{(0)}(0)+2\omega_0^2}\left[\frac{\pi}{2}-2\right].$$

The quartic equation (A 5) is solved numerically and the appropriate real root of the equation then gives $K_u^{(1)}(0)$, and hence $K_u^{(2)}(0)$.

References

[1] Williams, G., 1978, *Chem. Soc. Rev.*, **7**, 89.
[2] Steele, W. A., 1976, *Adv. chem. Phys.*, **34**, 1.
[3] Evans, M. W., 1977, *Dielectric and Related Molecular Processes*, Vol. 3 (Senior reporter : M. Davies) (The Chemical Society), pp. 1–44.
[4] (a) Evans, M. W., 1977, *Adv. Molec. Rel. Int. Processes*, **10**, 203. (b) Rowlinson, J. S., and Evans, M. W., 1975, *A. Rep. chem. Soc.* A, p. 5.
[5] Brier, P. N., and Perry, A., 1978, *Adv. Molec. Rel. Int. Processes*, **13**, 1.
[6] Davies, M., 1970, *A. Rep.* A, **67**, 65.
[7] (a) Gordon, R. G., 1966, *J. chem. Phys.*, **44**, 1830. (b) Gordon, R. G., 1968, *Adv. magn. Reson.*, **3**, 1. (c) McClung, R. E. D., 1972, *J. chem. Phys.*, **57**, 5478.
[8] (a) Evans, G. J., Evans, M. W., and Reid, C. J., 1978, *J. chem. Soc., Faraday II*, **74**, 343. (b) Reid, C. J., Yadav, R. A., Evans, G. J., and Evans, M. W., 1978, *J. chem. Soc., Faraday II*, **74**, 2143.
[9] Mori, H., 1965, *Prog. theor. Phys.*, **33**, 423.
[10] (a) Evans, G. J., and Evans, M., 1976, *J. chem. Soc., Faraday II*, **72**, 1169. (b) Evans, G. J., and Evans, M., 1976, *J. chem. Soc., Faraday Trans.*, **72**, 1901. (c) Davies, G. J., Evans, G. J., and Evans, M., 1977, *J. chem. Soc., Faraday II*, **73**, 1071. (d) Evans, G. J., and Evans, M., 1977, *Chem. Phys. Lett.*, **45**, 454.
[11] Brot, C., 1975, *Dielectric and Related Molecular Processes*, Vol. 2 (Senior reporter : M. Davies) (The Chemical Society), pp. 1–47.
[12] (a) Lindenberg, K., and Cukier, R. I., 1975, *J. chem. Phys.*, **62**, 3271. (b) Frenkel, D., Wegdam, G. H., and van der Elsken, J., 1972, *J. chem. Phys.*, **57**, 2691.
[13] Streett, W. B., and Tildesley, D. J., 1978, *J. chem. Phys.*, **68**, 1275.
[14] (a) Yarwood, J., James, P. L., Döge, G., and Arndt, R., 1979, *Faraday Discussion* No. 66 (The Chemical Society), paper No. 19. (b) Evans, M. W., and Evans, G. J. (unpublished data). (c) Yarwood, J., James, P. L., Birch, J. R., and Afsar, M. N. (in preparation).
[15] (a) Berne, B. J., and Harp, G. D., 1971, *Physical Chemistry—An Advanced Treatise*, Vol. VIIIB, edited by H. Eyring, D. Henderson and W. Jost (Academic Press), pp. 540–713. (b) Berne, B. J., and Harp, G. D., 1970, *Adv. chem. Phys.*, **17**, 63.
[16] Davies, A. R., and Evans, M. W., 1978, *Molec. Phys.*, **35**, 857.
[17] (a) Calderwood, J. H., and Coffey, W. T., 1977, *Proc. R. Soc.* A, **356**, 269. (b) Coffey, W. T., Evans, G. J., Evans, M. W., and Wegdam, G. H., 1978, *J. chem. Soc., Faraday II*, **74**, 310. (c) Coffey, W. T., and Evans, M. W., 1978, *Molec. Phys.*, **35**, 975. (d) Evans, G. J., and Evans, M. W., 1978, *J. Chim. phys.*, **75**, 21.
[18] Morita, A., 1978, *J. Phys.* D, **11**, L9, L1.

[19] Budó, A., Fischer, E., and Miyamoto, S., 1939, *Phys. Z.*, **40**, 337.
[20] (a) Berne, B. J., and Montgomery, J. A., 1976, *Molec. Phys.*, **32**, 363. (b) Chandler, D., 1974, *J. chem. Phys.*, **60**, 3508.
[21] Bliot, F., Abbar, C., and Constant, E., 1972, *Molec. Phys.*, **24**, 241.
[22] Drawid, M., and Halley, J. W., 1977, *J. Phys. Chem. Solids*, **38**, 1269.
[23] (a) Bliot, F., and Constant, E., 1973, *Chem. Phys. Lett.*, **18**, 253; 1974, *Ibid.*, **29**, 618. (b) Evans, G. J., 1977, *J. chem. Soc., Faraday II*, **73**, 729. (c) Evans, M. W., 1976, *Spectrochim. Acta* A, **32**, 1259. (d) Davies, G. J., and Evans, M. W., 1976, *J. chem. Soc., Faraday II*, **72**, 1206. (e) Evans, G. J., and Evans, M. W., 1977, *Chem. Phys. Lett.*, **45**, 454.
[24] Desplanques, P., 1974, Thèse d'Etat, Univ. Lille.
[25] Damle, P. S., Sjölander, A., and Singwi, K. S., 1968, *Phys. Rev.*, **165**, 277.
[26] Hermans, F., Kestermont, E., van Loon, R., and Finsy, R., *3rd International Conference on Submillimetre Waves and their Applications*, Abstracts, p. 1026.
[27] (a) Coffey, W. T., 1979, *Molec. Phys.*, **37**, 473. (b) Davies, A. R. (personal communication).
[28] Gerschel, A., Darmon, I., and Brot, C., 1972, *Molec. Phys.*, **23**, 317.
[29] Dill, J. F., Litovitz, T. A., and Bucaro, J. A., 1975, *J. chem. Phys.*, **62**, 3839.
[30] Chamberlain, J., 1968, *Chem. Phys. Lett.*, **7**, 464.
[31] Martin, D. H., and Puplett, E., 1969, *Infrared Physics*, **10**, 105.
[32] Barojas, J., Levesque, D., and Quentrec, B., 1973, *Phys. Rev.* A, **7**, 1092.
[33] Griffiths, J. E., 1977, *Vibrational Spectra and Structure*, Vol. 6, edited by J. R. Durig (Elsevier).
[34] Griffiths, J. E., 1973, *J. chem. Phys.*, **75**, 751.
[35] Bartoli, F. J., and Litovitz, T. A., 1972, *J. chem. Phys.*, **56**, 413.
[36] Mansingh, K., and A., 1964, *J. chem. Phys.*, **41**, 827.
[37] Yarwood, J., Döge, G., and Arndt, R., 1977, *Chem. Phys.*, **25**, 387.
[38] Aman da Costa, A. M., Norman, M. A., and Clarke, J. H. R., 1975, *Molec. Phys.*, **29**, 191.
[39] Whittenburg, S. L., and Wang, C. H., 1977, *J. chem. Phys.*, **66**, 4255. Lyerla, J. R., Grant, D. M., and Wang, C. H., 1971, *J. chem. Phys.*, **55**, 4676.
[40] Bull, T. E., 1975, *J. chem. Phys.*, **62**, 222.
[41] Jones, D. R., Anderson, H. C., and Pecora, R., 1975, *Chem. Phys.*, **9**, 339.
[42] Breuillard-Alliot, C., and Soussen-Jacob, J., 1974, *Molec. Phys.*, **28**, 905.
[43] Rothschild, W. G., 1972, *J. chem. Phys.*, **57**, 991 and references therein.
[44] McClung, R. E. D., 1969, *J. chem. Phys.*, **51**, 3842; 1971, *Ibid.*, **54**, 3248; 1971, *Ibid.*, **55**, 359; 1972, *Ibid.*, **57**, 5478.
[45] Pardoe, G. W. F., 1969, Ph.D. Thesis, Univ. Wales.
[46] van Aalst, R. M., van der Elsken, J., Frenkel, D., and Wegdam, G. H., 1972, *Faraday Symposium Chem. Soc.*, No. 6, p. 94. Kroon, S. G., and van der Elsken, J., 1967, *Chem. Phys. Lett.*, **1**, 285.
[47] Evans, M. W. (unpublished data).
[48] Eloranta, J., and Kadaba, P. K., 1971, *Mater. Sci. Engng*, **8**, 203.
[49] Bulkin, B. J., 1969, *Helv. chim. Acta*, **52**, 1348.